

Improved dead reckoning using caster wheel sensing on a differentially steered 3-wheeled autonomous vehicle

David C. Conner^{*a}, Philip R. Kedrowski^a, Charles F. Reinholtz^a, John S. Bay^b
^aDepartment of Mechanical Engineering, Virginia Tech, Blacksburg, VA 24060
^bRaytheon Company, Falls Church, Virginia 22042

ABSTRACT

A differentially steered three-wheeled vehicle has proven to be an effective platform for outdoor navigation. Many applications for this vehicle configuration, including planetary exploration and landmine/UXO location, require accurate localization. In spite of known problems, odometry, also called dead reckoning, remains one of the least expensive and most popular methods for localization. This paper presents the results of an investigation into the benefits of instrumenting the rear caster wheel to supplement the drive wheel encoders in odometry. A linear observer is used to fuse the data between the drive wheel encoders and the caster data. This method can also be extended using the standard form of the Kalman filter to allow for noise. Improvements in position estimation in the face of common problems such as slip and dimensional errors are quantified.

Keywords: Sensor fusion, Kalman filter, dead reckoning, autonomous vehicles, mobile robots

1. INTRODUCTION

This paper builds upon work accomplished by the Autonomous Vehicle Team at Virginia Tech. Each year the team develops a vehicle for entry into the annual Intelligent Ground Vehicle Competition (IGVC). The newest vehicle, dubbed Navigator, was designed for entry into the 8th annual IGVC, held July 8-10, 2000, in Orlando, Florida¹. This vehicle, shown in Figure 1, is a 3-wheeled differentially driven vehicle. The two large front wheels provide both drive and steering, while the third wheel is free to rotate about its vertical axis. This configuration allows for the capability of zero radius turns and leads to an exceedingly nimble vehicle, without the ground damage caused by skid steering.

1.1 Motivation

Many of the proposed applications for this type of vehicle, from exploration and mapping to landmine detection and removal, require some type of localization¹.

The most common form of localization is odometry or dead reckoning². Unfortunately, odometry has several well-known limitations, due mostly to kinematic inaccuracies and slip. Odometry errors on a typical mobile robot can become so predominant that position estimates are unreliable after as little as 10 meters of travel.³ Because the error associated with odometry grows unbounded as the vehicle moves, some sort of external localization is required for accurate position tracking. Common methods of external localization include the use of engineered landmarks or beacons, visual landmark recognition, or global positioning system (GPS) sensors. Each of these methods for external localization adds to the expense of the



Figure 1. Navigator – a 3-wheeled differentially driven autonomous vehicle

* Correspondence: Email: dconner@cmu.edu; WWW: <http://www.cs.cmu.edu/~dconner>;

Address: David Conner, Robotics Institute, Carnegie Mellon University, 5000 Forbes Ave, Pittsburgh, PA 15213
Telephone: 412.268.8809 Fax: 412.268.5571

system, and suffers particular shortcomings in different environments. For example, GPS does not work for planetary exploration.⁴

This paper investigates a method for improving the position estimates obtained from odometry by using supplemental sensors. While not eliminating the need for explicit localization, the improved position estimates allow the vehicle to more closely follow the desired path. The improved path following in turn allows for less frequent explicit localization. Other systems have been proposed for improving the odometry estimates.⁴⁻⁹ Most of these systems use either special sensors or detailed models of sensor parameters to allow for the improvements. This paper investigates the use of encoders, which are less expensive than other methods, to instrument the caster wheel in order to obtain heading and velocity data. This additional data will be fused with the data from the drive wheel encoders using a standard linear observer. While this method can be expanded using Kalman filtering techniques, the focus of this paper is on the data fusion and compensation of systematic and non-systematic errors that lead to the inaccuracies associated with dead reckoning.

1.2 Review

Odometry measurements suffer from two major sources of errors, which have been classified as systematic and non-systematic.⁵ Systematic errors are those that are inherent in the vehicle, and are independent of the environment.⁵ Unequal wheel diameters and uncertainty about the effective wheelbase are the dominant forms of systematic error. The vehicle kinematic equations, developed in section 2.1, are highly dependant on these parameters. Since the vehicle position estimate is calculated directly from the wheel encoder measurements using the kinematic equations, errors in these parameters directly affects the accuracy of localization using odometry. Although calibration techniques have been developed to measure and compensate for systematic errors, some of the parameters change with time due to shifts in vehicle loading or changes in pneumatic tire pressure.³ Because of these changes in the systematic parameters, the errors associated with these parameters cannot be completely eliminated using calibration.⁵ Other systems have used passive and unloaded wheels equipped with encoders to reduce some of these effects. Typically these passive wheels are also sharp edged to reduce the wheel base uncertainty.

Non-systematic errors are those errors associated with the vehicle environment.⁵ These are typically associated with ground unevenness and roughness, bumps, and wheel slippage. Because these errors are random, the vehicle cannot be calibrated to handle them. Because odometry is based on a relation between wheel rotations and vehicle movement, when a wheel rolls over a bump, the relationship is changed. Because the odometry calculations do not take this transient change into account, the position estimates accrue an error. The most dominant error is that of the vehicle-heading estimate, because subsequent position estimates are based on the heading estimate. This causes errors in position estimation to grow unbounded as the vehicle moves away from the original source of the heading error. Wheel slippage also induces the same types of errors by violating the kinematic constraints between wheel rotations and vehicle movement.

Borenstein et al have proposed hardware solutions to detecting the errors associated with both systematic and non-systematic errors.^{5,6,7} In one method, two vehicles are linked together with a compliant linkage.^{6,7} The linkage is instrumented to measure the relative displacements, both linear and angular, between the vehicles. The vehicles use an algorithm known as *Internal Position Error Correction* (IPEC) to detect odometry errors in one vehicle using the sensors in the linkage and the action of the one vehicle relative to the other. By identifying the type of errors based on the *Growth-Rate Concept*, the vehicles can mutually identify and correct for orientation errors before substantial lateral errors accumulate. Additionally, the IPEC method can also detect and correct for systematic errors. Use of the IPEC has shown to improve odometry estimates by up to two orders of magnitude over traditional dead reckoning.⁵ This concept has been extended to work with traditional vehicles by using a Smart Encoder Trailer (SET). The vehicle tows the SET behind itself, which allows the SET to perform the same function as the compliant linkage. The SET is equipped with a set of encoders to act as the second vehicle in the IPEC.

Other researchers have proposed different hardware measures to improve position estimates. Some have supplemented the odometry with inertial measurements such as gyroscopes and accelerometers.³ Unfortunately, these methods have been found to be subject to substantial drift. Roumeliotis and Bekey proposed a system which used a gyroscope and sun sensor to improve the position estimation of simulated Mars rover.⁴ The system used frequent updates from the vehicle data, along with an less frequent reading from the sun sensor. Improvements of up to 40 % over traditional odometry were found in simulation.

In addition to the hardware enhancements, researchers have investigated several theoretical techniques for improving odometry estimates, with the most prevalent methods being based upon the Kalman filter.^{2,4,9} The Kalman filter is a form of linear observer that provides optimal state estimates in the presence of noise.^{9,10} The development of the Kalman filter requires the noise to be uncorrelated, stationary, with a zero-mean and Gaussian distribution. For noise of this type, the Kalman filter provides a state estimate that is optimal in the sense of minimizing the squared error between the actual state and the estimated state. If the noise distribution is not Gaussian, the Kalman filter provides the best estimate for a linear state estimator. The Kalman filter has been extended to non-linear systems in the form of the Iterated Extended Kalman Filter (IEKF).^{4,9}

While the Kalman filter provides an optimal estimate of the states in the presence of noise, its performance comes at a cost.⁹ Calculation of the time varying Kalman gains requires an updated estimate of the covariance matrix, which has a non-trivial computational burden. Furthermore, the optimality of the technique is based on a specific model of the noise. For systems that are under the influence of bias errors or correlated noise, the Kalman filter is not optimal. For this reason, a simple form of linear observer is the focus of this paper. This allows the focus to be on the motivation for instrumenting the rear caster wheel, without obscuring the issue with a discussion of noise models and statistics.

This paper first develops the necessary kinematic equations for Navigator’s three-wheeled configuration (Figure 1), then discusses the development of the sensor model used in formulation of the linear observer. Further, comparisons between two different sensor models are made, along with a discussion of the observer gain calculations. Finally, a comparison of the simulation results is given.

2. VEHICLE MODELS

In order to develop the equations used for odometry and the linear observer, the kinematic relationships between wheel rotations and vehicle movement must be developed. Furthermore, to increase the accuracy of the simulations a dynamic model is needed. This section discusses the development of the kinematic and dynamic models used to investigate the usefulness of rear caster wheel instrumentation.

2.1 Kinematic Model

The kinematic relationships for the vehicle are developed based on a planar model of the vehicle¹. Figure 2 shows the vehicle plan view with the vehicle dimensions marked. The vehicle steers by rotating one wheel farther than the other, as shown in Figure 3 by the arcs s_a and s_b . As the vehicle moves in the ground plane, the vehicle rotates about the instant center O. This allows the rigid body vehicle, which is both translating and rotating in the plane, to be described as purely rotating about point O. The instant center, O, changes with time as the vehicle steers.

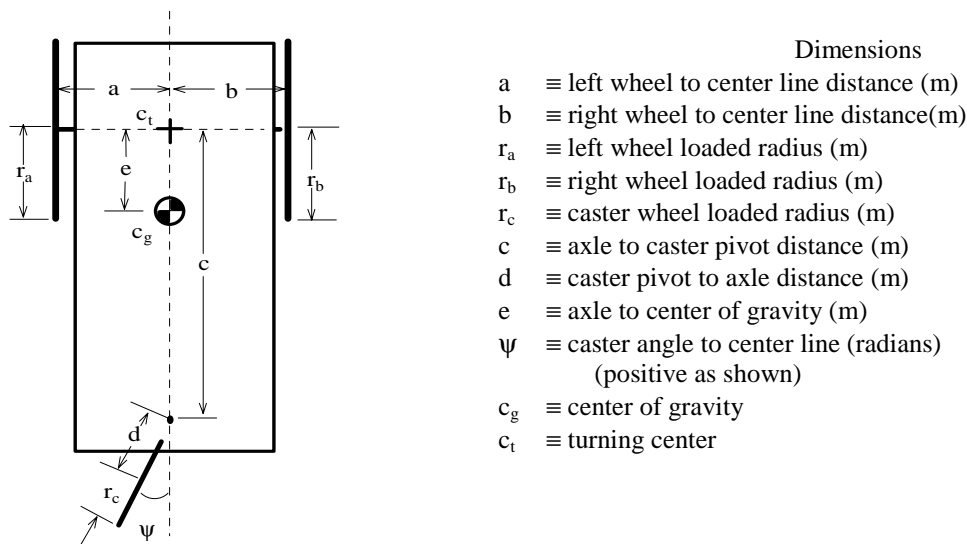


Figure 2. Plan View of Vehicle

Because s_a and s_b are related to the drive wheel rotations, θ_a and θ_b , by their respective wheel radii, the movement of the vehicle in the plane can be described relative to the rotations of the wheels. By applying principles of geometry and then differentiating, it can be shown¹ that the angular velocity (i.e. rate of change of heading) of the vehicle is given by

$$\dot{\phi} = \dot{\beta} = \frac{r_b \dot{\theta}_b - r_a \dot{\theta}_a}{a + b} \quad (1)$$

The speed of the vehicle, v_v , along the path traveled by the turning center, is given by a weighted average of the speeds along the arcs s_a and s_b . This relationship is calculated as

$$v_v = \frac{a r_a \dot{\theta}_a + b r_b \dot{\theta}_b}{a + b} \quad (2)$$

For the normal case, where a and b are equal, this equation reduces to the numerical average given by

$$v_v = \frac{r_a \dot{\theta}_a + r_b \dot{\theta}_b}{2} \quad (3)$$

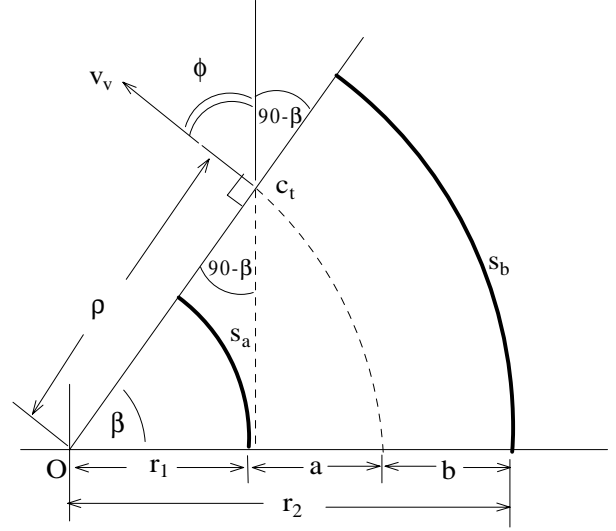


Figure 3. Differential Steering

Because the vehicle is subject to non-holonomic constraints, the position cannot be determined by integrating the wheel velocities alone. However, if equation 1 is numerically integrated to determine the vehicle heading, and equation 3 is used to determine speed, the position can be estimated by numerically integrating the component velocities. If a global coordinate system is chosen, where positive ϕ is measured in the right-hand sense from the y-axis, the vehicle component velocities are given by

$$v_x = -v_v \sin(\phi) \quad (4)$$

$$v_y = v_v \cos(\phi) \quad (5)$$

Although the equations for the component velocities are non-linear and cannot be linearized due to the potentially large heading angle ϕ , the equations for the vehicle speed and rate of change of heading (turning rate) are linear¹. This allows for a linear model to be developed which calculates the vehicle speed and heading. Given the correct values for speed and heading, the vehicle position can be estimated by numerically integrating the component velocities. This is known as dead reckoning. Unfortunately, the calculation of speed and heading are subject to the errors caused by kinematic inaccuracies mentioned in section 1.2.² Errors in the calculation of speed and heading lead to unbounded errors in the position estimation.

Because the equations for vehicle speed and turning rate are linear with respect to the wheel angular velocities, a linear control law based on the kinematic geometry of the vehicle can be developed. Given a desired velocity v_{ref} and a desired turning rate $\dot{\phi}_{ref}$, equations 1 and 3 can be used to calculate the required wheel angular velocities as

$$\left(\dot{\theta}_a \right)_{ref} = \frac{2v_{ref} - \dot{\phi}_{ref}(a+b)}{2r_a} \quad (6)$$

$$\left(\dot{\theta}_b \right)_{ref} = \frac{2v_{ref} + \dot{\phi}_{ref}(a+b)}{2r_b} \quad (7)$$

Since this paper proposes to improve the position estimate by adding instrumentation to the rear caster wheel, the kinematic relationship between the vehicle motion and the rear caster must also be developed.¹ Figure 4 shows the geometric relationship between the caster wheel and the instantaneous vehicle motion. The caster wheel ground speed is calculated by

$$v_c = r_c \dot{\theta}_c \quad (8)$$

where, r_c is the radius of the caster wheel and $\dot{\theta}_c$ is the angular velocity of the caster wheel. Since the instantaneous vehicle speed, v_v , is along the vehicle centerline, the following relationship holds:

$$v_v = v_c \cos(\Psi) = r_c \dot{\theta}_c \cos(\Psi) \quad (9)$$

Also, the turning rate of the vehicle is given by

$$\dot{\phi} = \frac{v_c}{c} \sin(\Psi) = \frac{r_c}{c} \dot{\theta}_c \sin(\Psi) \quad (10)$$

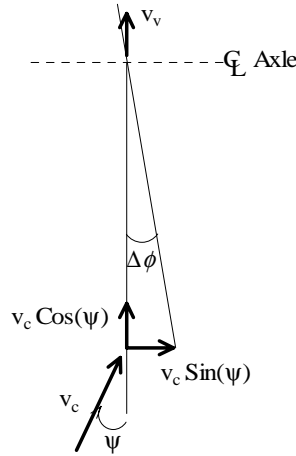


Figure 4. Caster wheel geometric relationship to vehicle motion

2.2 Dynamic Model

In order to test the value of providing the supplemental measurements, a dynamic model has been developed which allows the theory to be tested in simulation.¹ Both linear and non-linear models have been developed using analytical dynamics. The effects of the caster wheel upon the vehicle dynamics are pronounced when the vehicle is moving in such a way that the caster wheel must rotate about its vertical axis quickly. For example, if the vehicle attempts a zero radius turn after previously traveling forward high initial side force is required in order to rotate the caster wheel into a position perpendicular to the vehicle. Once the caster wheel achieves this position, the side force drops significantly and nonlinearly. The linear model is inadequate to model the vehicle behavior in this case. However, during gradual turns, with a radius of curvature of several meters, the linear model predicts the vehicle behavior well.

In addition to the vehicle dynamics, the simulation was programmed in such a way as to simulate the vehicle control system, which uses an implementation of the discrete PID algorithm¹. The reader is referred to reference 1 for a complete development of the model, and experimental validation. Figure 5 shows one of the validation tests comparing the actual vehicle acceleration and deceleration with that of both linear and non-linear model.

As shown by Figure 5, both the linear model and the non-linear model capture the essential dynamics of the actual vehicle for this simple type of motion. Because the linear model, which neglects the caster wheel torque effects, has a much faster execution time, the simulations in this paper were conducted using the linear model. Because the sensor observer model uses feedback of the actual wheel rotations, the non-linear effects due to the caster assembly rotation are not required for the observer.

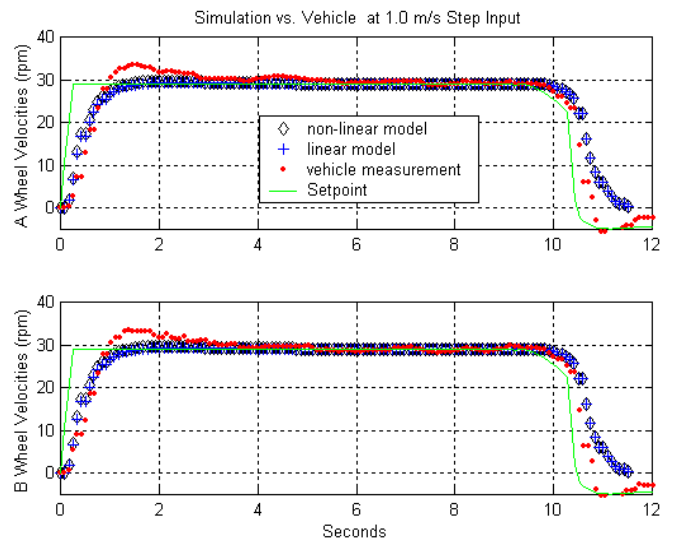


Figure 5. Model verification test

3. SENSOR MODELS

This section details the development of the sensor models that form the foundation of the discrete linear observer used to fuse the sensor data for improvement of vehicle position estimates. Typical observers are based on the dynamic model of the system; unfortunately the parameters of this system are known to vary substantially with changes in ground conditions. For this reason, two different sensor models are compared. Both models have the same basic form, with the estimated state and output vectors of the form

$$\hat{x} = \begin{bmatrix} \hat{\theta}_a \\ \hat{\theta}_b \\ \hat{\theta}_a \\ \hat{\theta}_b \end{bmatrix} \quad \text{and} \quad \hat{y} = \begin{bmatrix} \hat{\theta}_a \\ \hat{\theta}_b \\ \hat{v}_v \\ \hat{\phi} \end{bmatrix}$$

where the $\hat{\cdot}$ denotes the observed or estimated value, corresponding to the actual system vectors.

The output vector for both models corresponds to the sensed values from the encoder feedbacks, and the velocity and turning rate. The caster wheel sensors include the caster assembly angle and the caster wheel rotation, which are processed using equations 9 and 10. Equations 9 and 10 are non-linear, and as such, preclude the use of a linear observer. However, if one preprocesses the actual sensed values of $\dot{\theta}_c$ and ψ using equations 9 and 10 to yield ‘‘sensed’’ values of v_c and $\dot{\phi}$, a linear observer model can be constructed.¹ For the observer, both sensor models have the same output matrix of the form

$$\hat{y}_k = C\hat{x}_k, \quad \text{where} \quad C = \begin{bmatrix} 0 & 0 & 1 & 0 \\ 0 & 0 & 0 & 1 \\ 0 & 0 & \frac{r_a}{2} & \frac{r_b}{2} \\ 0 & 0 & \frac{-r_a}{(a+b)} & \frac{r_b}{(a+b)} \end{bmatrix}$$

For the output model, the parameters are set according their theoretical values, while the dynamic model uses the parameters that have been perturbed with systematic errors.

3.1 Plant Sensor Model

The first sensor model is a simplified system based on the system dynamic model. While the motor current inputs are included, the effects of the rolling friction are neglected since this component is subject to substantial variation. Furthermore, the simulations in this paper perturb the values of the dynamic values by 10% to represent the uncertainty involved in modeling the actual vehicle. The linear observer has the form $\hat{x}_{k+1} = A\hat{x}_k + B\bar{u}_k + L(\bar{y} - C\bar{x}_k)$. For the vehicle discussed in this paper, A and B are equal to

$$A = \begin{bmatrix} 1 & 0 & 0.0209 & 0 \\ 0 & 1 & 0 & 0.0209 \\ 0 & 0 & 0.9945 & -0.237e^{-2} \\ 0 & 0 & -0.237e^{-2} & 0.9945 \end{bmatrix} \quad B = \begin{bmatrix} 0.427e^{-4} & 0.186e^{-4} \\ 0.186e^{-4} & 0.427e^{-4} \\ 0.406e^{-2} & 0.177e^{-2} \\ 0.177e^{-2} & 0.406e^{-2} \end{bmatrix}$$

The development of the linear observer requires that the system is observable. On investigation the system as given is shown not to be observable. However, the system is in the observable canonical form. Therefore, the 2x2 sub-matrix in the lower right corner of the A matrix is observable, and the observer can be partitioned into the following form:

$$\hat{x}_{k+1} = \begin{bmatrix} A_{no} & A_{12} \\ 0 & A_o \end{bmatrix} \hat{x}_k + \begin{bmatrix} B_{no} \\ B_o \end{bmatrix} \bar{u} + \begin{bmatrix} 0 \\ L \end{bmatrix} (\bar{y} - [0 \ C_2] \bar{x}_k) \quad (11)$$

This form of the observer can be simplified as

$$\hat{\bar{x}}_{k+1} = \begin{bmatrix} A_{no} & A_{12} \\ 0 & A_o - LC_2 \end{bmatrix} \hat{\bar{x}}_k + \begin{bmatrix} B_{no} \\ B_o \end{bmatrix} \bar{u} + \begin{bmatrix} 0 \\ L \end{bmatrix} \bar{y} \quad (12)$$

The gain matrix L is typically chosen so that the error for the observable states given by $\bar{x}_o - \hat{\bar{x}}_o$ is asymptotically stable. By inspection the matrix L is a 2x4 matrix, which gives 8 parameters, which are used to arbitrarily place 2 poles in the closed loop A-matrix shown in equation 12. This gives a significant amount of freedom in choosing the gains L. We will return to this discussion after the alternate sensor model is introduced.

3.2 Simplified Sensor Model

The second sensor model test is a greatly simplified system, where the state estimates are only driven by the error between the measured values and the estimated output. In this form the current inputs are ignored. The observer has the form

$$\hat{\bar{x}}_{k+1} = \begin{bmatrix} 1 & 0 & T_s & 0 \\ 0 & 1 & 0 & T_s \\ 0 & 0 & \tau & 0 \\ 0 & 0 & 0 & \tau \end{bmatrix} \hat{\bar{x}}_k + \begin{bmatrix} 0 \\ L \end{bmatrix} (\bar{y} - [0 \ C_2] \bar{x}_k) \quad (13)$$

Again this system is in the observable canonical form, and can be simplified, as was done going from equation 11 to 12. Once again, the system has 8 parameters to choose for the gain matrix L to place 2 poles.

3.3 Gain Selection

The linear observers developed above require the calculation of an observer gain matrix, L. These gains are calculated such that the error between the predicted output and the sensed output decays over time. Because of the under constrained nature of the problem of calculating 8 parameters to fit 2 poles, the typical pole placement techniques are less helpful. The null space for the calculation is large for a given set of poles, and therefore requires additional insight into the problem. Two basic approaches are used in the simulations conducted in this work.

By taking advantage of the duality between observability and controllability, the observer gain design can be recast as a controller gain problem. For this task, the standard discrete form of the Linear Quadratic (LQ) minimization technique is used, with sub-matrix A_o^T and C_2^T serving in the role of A and B in the formulation. The development of this technique is beyond the scope of this paper, but is based on the minimization of a particular cost function using the discrete time matrix Ricatti equation.¹⁰ This method was chosen over the traditional Kalman filter design, because the LQ method is somewhat easier conceptually for users not trained in the stochastic basis for Kalman filter design. Furthermore, it is appropriate for the zero noise model that has been chosen for this simulation. The implementation of the LQ method involves defining two matrices, Q and R, and using the standard tools to solve the Ricatti equation to yield the set of gains that minimize the cost function defined by Q and R. For the calculations of the observer gains, the matrix Q weights the error states, while the matrix R weights the output feedback. Higher weights correspond to higher cost and therefore less desirable behavior. For the simulations conducted for this paper, the errors states were weighted quite heavily relative to the R-matrix applied to the feedbacks. The values of the R-matrix are chosen to weight the specific feedbacks relative to one another in order to bias the gains toward one sensor or another. In this work, the sensors are biased slightly toward the caster wheel since it is assumed that the caster wheel is not subject to slip, as are the drive wheels.

The second method is based upon physical insight into the problem, and involves a series of hand calculations. First, equations 6 and 7 are used to calculate estimates of the wheel speeds based on the vehicle speed and turning rate sensed by the caster wheel. Next, a weighting α can be defined which weights these estimates relative to the estimates provided by the wheel encoders. Finally, an overall weighting β can be defined between the new estimates and the previous state estimates.

By tuning the values for α , β , and τ , the gains can be calculated according to

$$L = \begin{bmatrix} \beta(1-\alpha) & 0 & \frac{\alpha\beta}{r_a} & -\alpha\beta \frac{(a+b)}{2r_a} \\ 0 & \beta(1-\alpha) & \frac{\alpha\beta}{r_b} & \alpha\beta \frac{(a+b)}{2r_b} \end{bmatrix} \quad (14)$$

By adjusting the relative weight α placed on the sensors, the system can be programmed to perform traditional dead reckoning based solely on the drive wheel sensors, or solely on the caster sensors, or on a linear combination of the different sensors. By adjusting β and τ , a valid set of closed loop poles can be calculated, which provide adequate filtering. With this insight, the simulations in the following section will compare the responses of a given set of gains to different types of errors, both systematic and non-systematic. For the simulations conducted in this paper, $\tau = 1.0$ and $\beta = 0.5$, and $\alpha = 0.7$.

Another point of discussion in the selection of the gains, is their effect on the response of the state estimates. Furthermore, the effect of noise in the sensor outputs on the state estimates should be discussed. Assume that the noise component is given as

$$\bar{y}_k = \tilde{y}_k + w_k \quad (15)$$

where the \sim denotes the ideal value and w_k is the noise. Equation 12 can be then be modified into the following form:

$$\hat{\bar{x}}_{k+1} = \begin{bmatrix} A_{no} & A_{12} \\ 0 & A_o - LC_2 \end{bmatrix} \hat{\bar{x}}_k + \begin{bmatrix} B_{no} & 0 & 0 \\ B_o & L & L \end{bmatrix} \begin{bmatrix} \bar{u} \\ \tilde{y} \\ w \end{bmatrix} \quad (16)$$

This allows the transfer function matrix to be calculated as

$$X(z) = \left[zI - \begin{bmatrix} A_{no} & A_{12} \\ 0 & A_o - LC_2 \end{bmatrix} \right]^{-1} \begin{bmatrix} B_{no} & 0 & 0 \\ B_o & L & L \end{bmatrix} \begin{bmatrix} U(z) \\ \tilde{Y}(z) \\ W(z) \end{bmatrix} \quad (17)$$

As is evident from the formulation, the characteristic equation of all of the transfer functions is based solely on the poles of the closed loop A-matrix. If the system has an initial B-matrix, the response of the state estimates to the inputs is related to this B-matrix. Likewise the L-matrix controls the response of the state estimates to the sensor feedbacks. Larger values in the L-matrix correspond to a larger response in the state estimates. However, since the sensor feedbacks will almost certainly include some noise component, the noise component will also be passed to the state estimates through the L matrix. Since the transfer functions between the true sensor feedbacks and the sensor noise are the same, it is imperative that they exhibit a strong high frequency roll off. This is one of the strong motivating factors for the development of the Kalman filter in the calculation of the observer gains. For this work, it is assumed that the signal to noise ratio in the sensor feedbacks is high enough that the impacts are negligible.

4. SIMULATION RESULTS

Although the problem that kinematic inaccuracies pose to localization using dead reckoning has previously been described, an example will help to clarify the problem and motivate the proposed solution.^{1, 2} Assuming equal wheel radii of 0.33 meters and a desired speed of 0.5 meters per second with a desired rotation rate of 1 degree per second, equations 6 and 7 are used to calculate the desired wheel speeds as

$$\begin{aligned} (\dot{\theta}_a)_{ref} &= 1.496 \text{ rad/sec} \\ (\dot{\theta}_b)_{ref} &= 1.535 \text{ rad/sec} \end{aligned}$$

The vehicle control system will regulate the wheel speeds based on the calculated reference speeds. This will result in a circle of diameter 57.3 meters being traveled over a 6-minute period. If all parameters are as specified, dead reckoning will estimate this exactly. However, if the radius of the right wheel is increased by 1 percent to 0.3333 meters, the actual speed and steering will change according to equations 1 and 2. In this example case, the actual speed is 0.5025 meters per second and the turning rate is 1.39 degrees per second. This results in a circle of diameter 41.4 meters being traveled in 4 minutes and 19 seconds. If the kinematic model is not updated to reflect the change in wheel diameters dead reckoning will still predict travel of the 57.3-meter diameter circle. Changes in wheel diameters, such as in this example, are especially prevalent in pneumatic tires, which are subject to over or under inflation.

The simulation code was developed and executed using Matlab®. The code included both the linear form of the dynamic model for the vehicle, and a simulation of the discrete control code that was used on the actual vehicle. Using the simulation code, several tests were conducted. For each test, a commanded speed setpoint and turning rate setpoint were specified. These setpoints were used to calculate the wheel angular velocity setpoints used by the control system. The dynamic model used the parameters for the actual vehicle, while the sensor model used the theoretical parameters. The remainder of this section discusses the results of the simulations.

4.1 Simulation of Systematic Errors

The first series of tests conducted assumed that the right tire was 1 percent larger than the left tire. In the first test, the vehicle was commanded to move in a straight line at 0.5 meter per second (i.e. zero turn rate). The result of this test is shown in Figure 6. As expected, the larger right wheel diameter forces the vehicle to turn to the left faster than expected for a given rotation. Because dead reckoning uses only the expected values for tire diameter, the vehicle “thinks” it is moving in a straight line. Without an external positioning system, the vehicle will quickly go off course. If, instead of using dead reckoning alone, the linear observer is implemented using the expected values a substantial improvement is seen. Because the caster wheel sensors provide another estimate of speed and steering, independent of the drive wheel encoder feedback, the observer is able to partially correct for the error in the wheel diameter estimation.

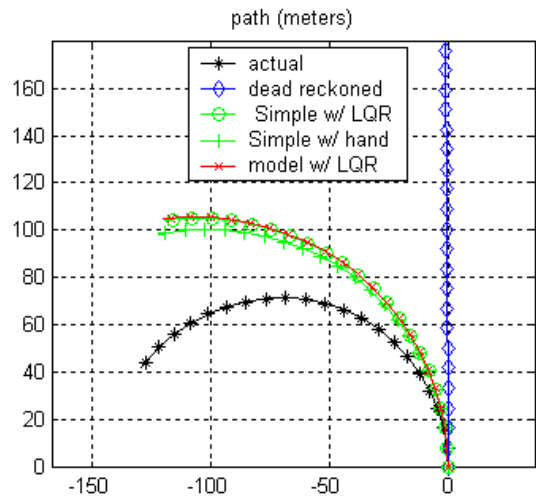


Figure 6. Straight-line motion with overinflated right tire

The next test mimicked the example given in the introduction to this section. A 0.5 meter per second speed with a 1.0 degree per second turn rate was commanded. The results of this test are shown in Figure 7. Again the augmentation using caster wheel sensing and a linear observer resulted in a significant improvement of the position estimation.

Another test was conducted where the vehicle turning rate varied sinusoidally between ± 10 degrees per second with a frequency of 0.005 radians per second. This result is shown in Figure 8. Again caster wheel augmentation using the linear observer results in a position estimate that is closer to the actual value than dead reckoning alone. However, because the heading does not match the actual heading, the error continues to grow unbounded. Therefore, although the linear observer improves the position estimation, it does not eliminate the need for an external positioning system.

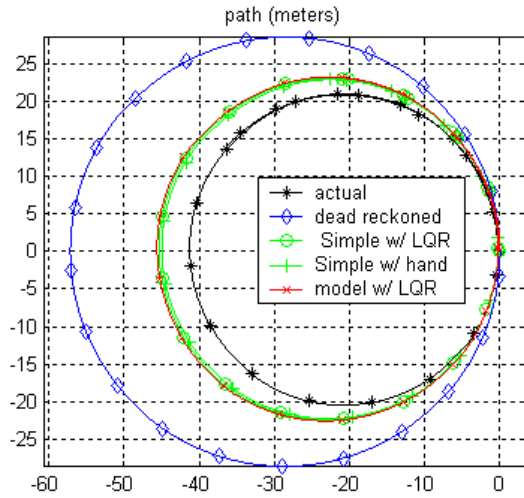


Figure 7. Turning motion with overinflated right tire

Another test was simulated using a 5 percent error on the wheel base measurement. In this case, a turning rate of 2 degrees per second was selected. As shown in Figure 9, the linear observer once again improved the position estimation dramatically.

For all of the tests the linear observer improved the position estimate in the face of systematic errors associated with the vehicle base or drive wheels. One may rightly ask to what extents will errors in the caster measurements impact the position estimates if the linear observer is implemented in place of standard dead reckoning. To answer this question, several simulations were analyzed. In these simulations, the caster placement measurements were perturbed, while the other vehicle parameters were left as specified. In the first of these simulations, the rear caster wheel diameter was perturbed yielding a 5 percent error in the speed and turning rate measurements. A portion of the results are shown in

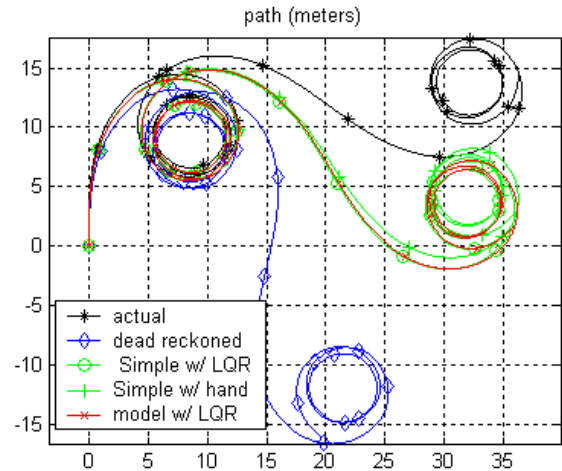


Figure 8. Oscillatory motion with overinflated right tire

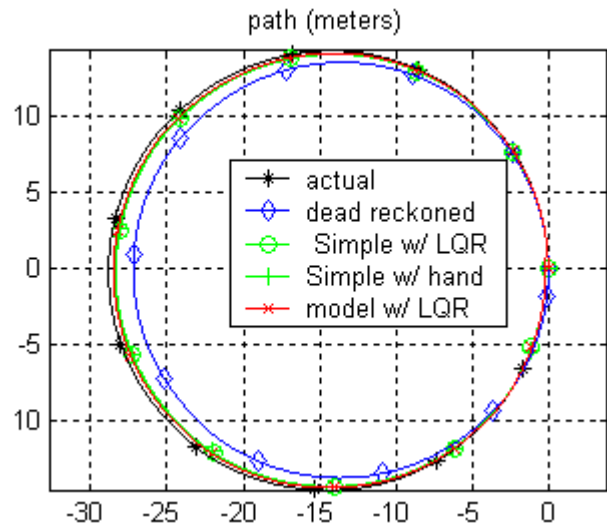


Figure 9. Turning motion with 5% wheelbase error

Figure 10. In the second simulation, the caster wheel pivot measurement was perturbed such that the turning rate measurement yielded a 5 percent error. A portion of this result is shown in Figure 11. As can be seen, the induced errors are small relative to the improvements shown with a smaller error in the drive wheel parameters. Therefore, although there is an inherent risk that systematic errors in the caster measurements will induce errors in the odometry where no systematic errors existed in the drive measurements, the scale of improvement to degradation and the scale of the relative measurements are such that the benefits generally outweigh the risks. When the effects of non-systematic errors, described in the next section, are included, the likelihood of significant degradation of performance is minimal.

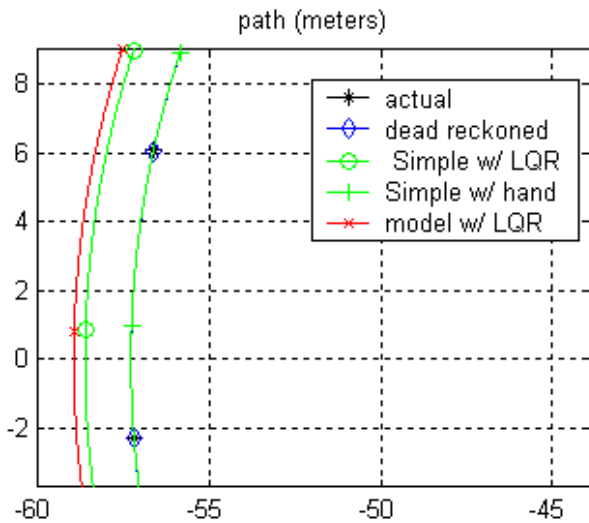


Figure 10. Induced error due to caster wheel error

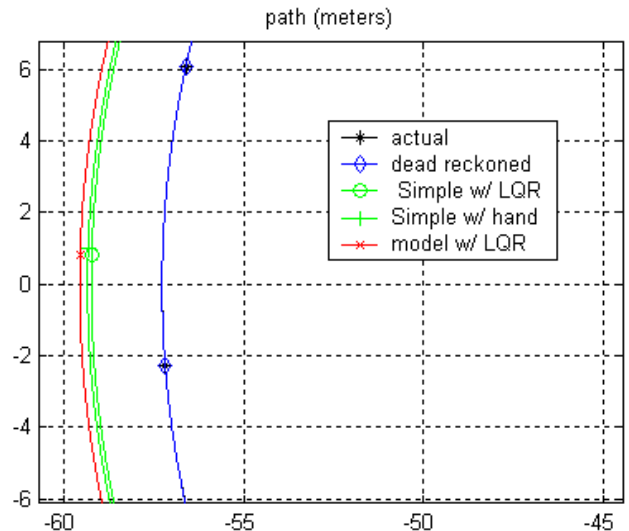


Figure 11. Induced error due to caster assembly position error

4.2 Simulation of Non-systematic Errors

The next class of errors simulated was for non-systematic errors. The simulations presented in this section are for drive wheel slippage, as would likely exist if the vehicle were traveling over loose materials. In this simulation, a straight-line move was commanded, and the left wheel was programmed to periodically slip. During slippage, the drive wheel encoders will register rotation, without a corresponding linear movement. The caster wheel encoders will only register the actual movement of the vehicle since the caster is a passive device. The slip is assumed to occur on the same wheel in order to magnify the effect on the system. Figure 12 shows the result of the simulated slip, with all systematic errors removed. Once again, the linear observer improves the position estimation substantially.

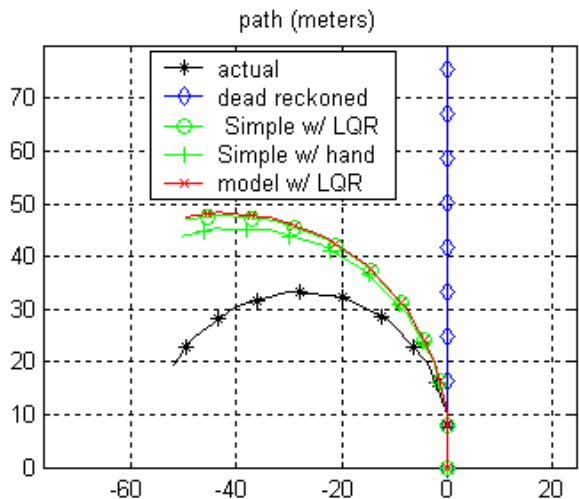


Figure 12. Straightline motion with left wheel slippage

4.3 Simulation of Sensor Noise

To test the susceptibility of the system to noise, the sensor feedbacks were each corrupted with a $\pm 5\%$ noise signal. The sensor noise elements were independent from one another. The encoder noise was also fed back into the drive wheel PID control loop, which caused the vehicle to move off of the desired path. The linear observer tracked this movement better than the dead reckoning based on the noisy data. The noise in this test did not degrade the performance of the linear observer substantially.

As a final example, Figure 13 shows a simulation combining the effects of systematic, non-systematic, and noise on the system. The linear observer is effective in filtering out the effects of all of the sources of error, and providing a better estimate of the position than dead reckoning alone. If it is assumed that the errors have a greater impact on the drive wheel encoders, the observer gains can be biased more toward the caster, which further improves the performance, as shown in Figure 14.

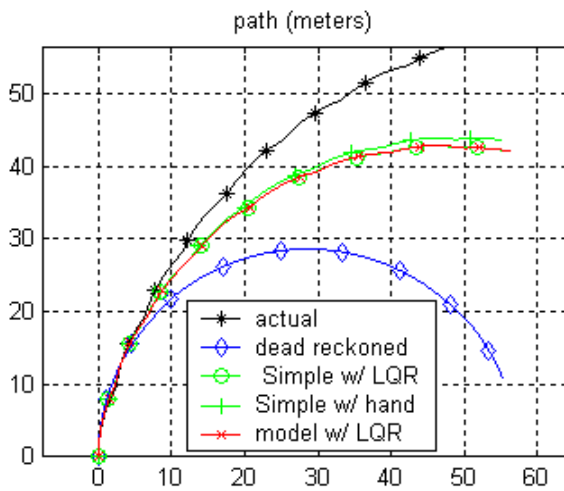


Figure 13. Combination noise, systematic, and non-systematic errors using a linear observer

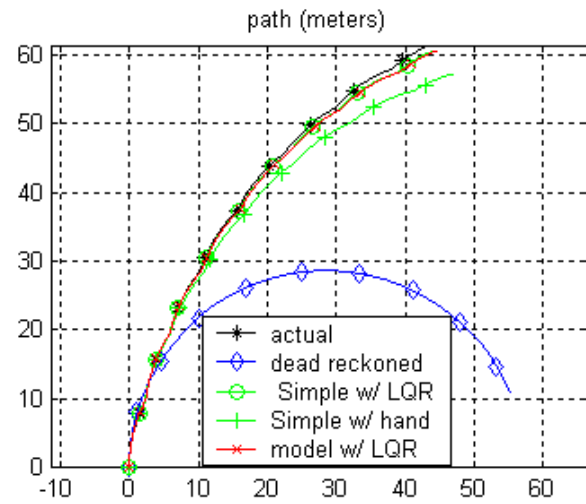


Figure 14. Combination of errors with linear observer biased toward caster sensors

5.0 Conclusion

This paper has demonstrated the effectiveness of a simple linear observer in fusing the data between drive wheel encoders and supplemental rear caster sensors. The performance of the observer model based on plant dynamics and the observer model based on simple error feedback was shown to be comparable. Furthermore, the calculations of the observer gains for the simple model using either a discrete LQ method or designer intuition has been shown to be effective. While not eliminating the need for periodic external localization, the simple linear observer has been shown to be effective in aiding the localization estimations and path tracking without the need for expensive hardware systems or computationally burdensome algorithms. While this method is not “optimal”, it is “good enough.”

REFERENCES

1. D. C. Conner, *Sensor Fusion, Navigation, and Control of Autonomous Vehicles*, Masters Thesis, Virginia Polytechnic Institute and State University, July 2000.
2. J. Borenstein, H.R. Everett, and L. Feng, *Navigating Mobile Robots: Systems and Techniques*, A K Peters, Ltd., Wellesley, MA, 1996.
3. J. Borenstein, and L. Feng, “Measurement and Correction of Systematic Odometry Errors in Mobile Robots.” *IEEE Journal of Robotics and Automation*, Vol 12, No 6, December 1996, pp. 869-880.
4. Roumeliotis, Stergios I, and Bekey, George A., “An Extended Kalman Filter for Frequent Local and Infrequent Global Sensor Data Fusion,” *Sensor Fusion and Decentralized Control in Autonomous Robotic Systems*, SPIE Vol. 3209, 1997 pp. 11-22.
5. J. Borenstein, “Internal Correction of Dead-reckoning Errors With the Smart Encoder Trailer.” *1994 International Conference on Intelligent Robots and Systems (IROS '94)*. Munich, Germany, September 12-16, 1994, pp. 127-134.
6. J. Borenstein, 1995, “Internal Correction of Dead-reckoning Errors With the Compliant Linkage Vehicle.” *Journal of Robotic Systems*, Vol. 12, No. 4, April 1995, pp. 257-273.
7. J. Borenstein, J. and D.K. Wehe, “Internal Correction of Odometry Errors with the OmniMate.” *Proceedings of the Seventh Topical Meeting on Robotics and Remote Systems*, Augusta, Georgia, April 27 - May 1st, 1997, pp. 323-329.
8. L.Kleeman, “Optimal estimation of position and heading for mobile robots using ultrasonic beacons and dead-reckoning”, *IEEE International Conference on Robotics and Automation*, Nice, France, pp 2582-2587, May 10-15 1992.
9. K.S. Chong, K.S. and L. Kleeman, L. “Accurate Odometry and Error Modeling for a Mobile Robot”, *Proceedings 1997 IEEE International Conference on Robotics and Automation*.
10. J.S. Bay, “Fundamentals of Linear State Space Systems”, McGraw-Hill, 1999.